In situ particle size measurements during crystallization processes using image analysis

Benoît Presles, Johan Debayle, Alain Rivoire, Jean-Charles Pinoli, Gilles Fevotte

XII ° Congrès de la Société Française de Génie des Procédés Pour relever les défis industriels du XXI° siècle A la croisée des Sciences et des Cultures, Marseille : France (2009)

In situ particle size measurements during crystallization processes using image analysis

PRESLES Benoît[1][2], DEBAYLE Johan[2] *, RIVOIRE Alain[3], PINOLI Jean-Charles[2], FEVOTTE Gilles[1][3]

[1] *Ecole Nationale Supérieure des Mines de Saint Etienne, Centre SPIN – Département GENERIC ; LPMG -UMR CNRS 5148, 158 Cours Fauriel - 42023 Saint-Étienne Cedex 2, France*

[2] *Ecole Nationale Supérieure des Mines de Saint Etienne, Centre CIS – Département DIM; LPMG -UMR CNRS 5148, 158 Cours Fauriel - 42023 Saint-Étienne Cedex 2, France*

[3] *Université Claude Bernard Lyon 1, LAGEP, UMR CNRS 5007 43 bd du 11 Novembre 1918, 69622 Villeurbanne Cedex, France*

Abstract:

The aim of this article is to present a new online image analysis based method for monitoring the Crystal Size Distribution (CSD) during batch solution crystallization processes. An in-situ imaging probe allows real time acquisition of 2D images of particles during the batch process. From these images, restoration and segmentation algorithms are performed in order to identify the particles. Thereafter, mathematical morphology enables to get geometrical and morphological particle measurements. Therefore, the CSD can be deduced all along the time of the crystallization process (until moderate solid concentration).

Keywords:

Crystal Size Distribution ; crystallization ; image analysis ; restoration ; segmentation.

I. Introduction

Solution crystallization processes are widely used in the process industry and notably the pharmaceutical industry as separation and purification operations and are expected to produce solids with desirable properties. In fact, the quality requirements for industrial crystallization processes are becoming more and more demanding, due to the pressure imposed by both the international competition and the consumers. In particular, as far as the pharmaceutical industry is concerned, the size and the shape of crystals are known to exhibit a considerable impact on the final quality of drugs (*i.e.* bioavailability, stability on storage, ease of processing, etc.).

As far as measuring the Crystal Size Distribution (CSD) is concerned, it is well established that conventional monitoring techniques, such as Laser Diffraction (LD), Ultrasonic Attenuation Spectroscopy (UAS) or focused-beam reflectance measurement (FBRM), do not provide reliable in-line estimates. Indeed, major difficulties arise from the in situ use of laser diffraction techniques since they require highly diluted samples of rather “ideal” particles. Indeed, “ideal” means here that the particles, in order to fit the theoretical models used to process LD measurements, should be as close as possible to spheres and exhibit rather simple distributions (*i.e.* multimodal distributions should be very cautiously analyzed). The main disadvantage of UAS is that it requires a large set of accurate data related to the liquid and particle phases (Mougin, 2003). Finally, the main disadvantage of FBRM is that it does not actually measures the CSD but the Chord Length Distribution (CLD). One should therefore convert the measured CLD into its corresponding CSD which is a very ill-posed problem, even

* Auteur à qui la correspondance devait être adressée : debayle@emse.fr

though successful applications have been demonstrated experimentally for spheres (Hukkanen and Braatz, 2003) and octahedrons (Worlitschek *et al.*, 2005). Various 2D image-based methods also exist (Zhou *et al.*, 2008) but most of them require assumptions about the shape of the particles and therefore cannot handle some crystallization phenomena like aggregate particles. Therefore, in order to bring new solution to this problem, the present study aims at monitoring crystallization processes through image analysis using a new in-situ 2D imaging probe.
In the first section, the experimental system used to observe the crystallization process will be explained. In the second section, the image analysis algorithm will be developed (image segmentation, restoration and measurement) and finally some characterization results will be presented before concluding.

II. Materials, experimental setup and image acquisition

The online system used for monitoring batch crystallization processes (Figure 1(a)) is a new in-situ probe: the "EZProbe sensor", which was developed in the University of Lyon. A light source transported by optical fiber illuminates in transmitted light a CCD camera which has the following specifications: 25 fps, resolution up to 4µm² per square pixel, 256 grey level images of size 640x480 pixels. An acquisition interface retrieves the video data, compresses it if necessary and sends it to a computer. This probe allows real time acquisition of 2D images of the particles generated during the crystallization process. This study was performed with citric acid particles crystallizing in water (Figure 1(b)).

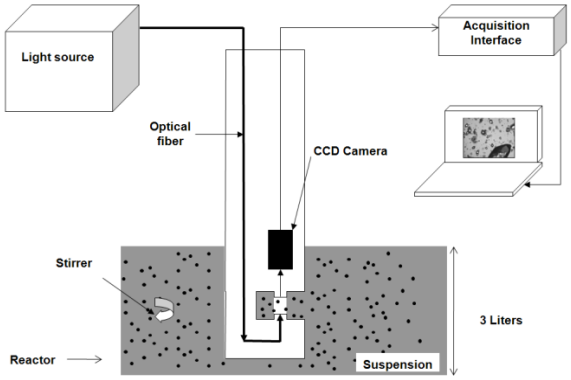

(a) Scheme of the acquisition system

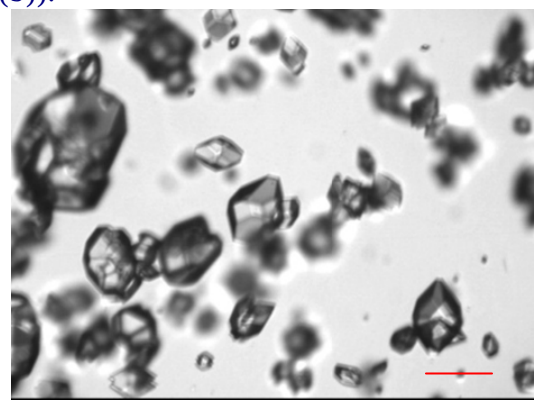

(b) 2D image of citric acid during crystallization

Figure 1: 2D image acquisition system

In order to characterize the particles, some difficulties have to be considered in the different image processing steps: 3D particles are actually projected into 2D images which obviously involves a significant loss of information, clustering, shape heterogeneity, anisotropy, particles outside the focal plane, etc. The next section aims at explaining the image analysis method which was designed so as to deal with those difficulties.

III. Image Analysis method

Firstly, for each image of the video sequence (Figure 2(a)), all particle regions are isolated as displayed in **Erreur ! Source du renvoi introuvable.**(Figure 2(b)). The method here consists in applying an algorithm based on the topography of the image: the watershed algorithm (Beucher, 1992) constrained by the h-minima (Vincent, 1993) of the image.
Secondly, by applying the automatic thresholding proposed by (Gonzalez and Woods, 2002) on each delimited area, the spatial support of each particle (*i.e.* the boundary of the particle) is detected ((Figure 2(c)). In addition, the particles in the focal plane (*i.e.* focused particles) are discriminated from those outside the focal plane (*i.e.* blurred particles) using a focus measurement (Yap and Raveendran, 2004), (Wee and Paramesran, 2007) calculated locally:

the variance focus measurement (Subbarao *et al.*, 1993) defined as $\frac{1}{MN}\sum_{x=1}^{N}\sum_{y=1}^{M} I(x,y)-\mu)^2$ where $I:\ \Omega \subset \mathbb{Z}^2 \rightarrow \mathbb{Z}$ is the grey level image ($x,\ y \in \Omega$), MxN is the size of the neighborhood and $\frac{1}{MN}\sum_{x=1}^{N}\sum_{y=1}^{M} I(x,y)$ ((Figure 2(c)).

Thirdly, in order to maximize the number of particles to be analyzed and to get an accurate particle characterization, a restoration step is performed ((Figure 2(d)): blurred particles (outside the focal plane) are restored by means of a blind deconvolution algorithm. Due to the presence of "ringing effects" in classical blind deconvolution algorithms (Kundur and Hatzinakos, 1996a), (Kundur and Hatzinakos, 1996b), (Fish *et al.*, 1995), a new blind deconvolution algorithm based on the image characteristics is developed. A detailed description of this algorithm can be found elsewhere (Presles *et al.*, 2009).

Finally, as the edge of the particles is now well defined, an accurate CSD analysis is possible. The CSD is computed using mathematical morphology on the binary image resulting from the restoration step. More precisely, an operation of granulometry which consists of an ensemble of opening by reconstruction of increasing size is performed (Soille, 2003). The particle size corresponds to the diameter of the largest disk contained in the shape.

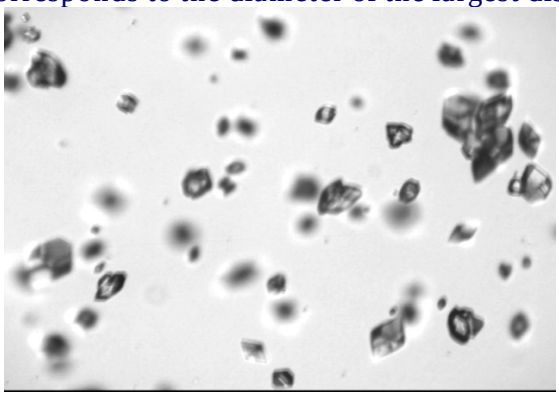

(a) Original image

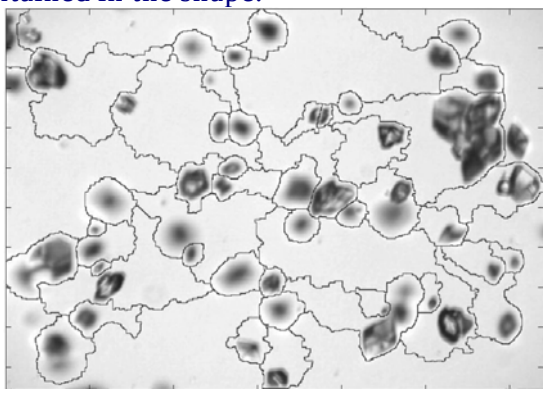

(b) Particle regions

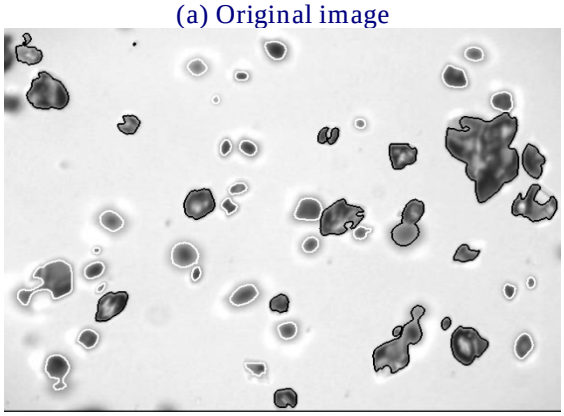

(c) Spatial support of each particle: in black, clean particles; in white blurred particles

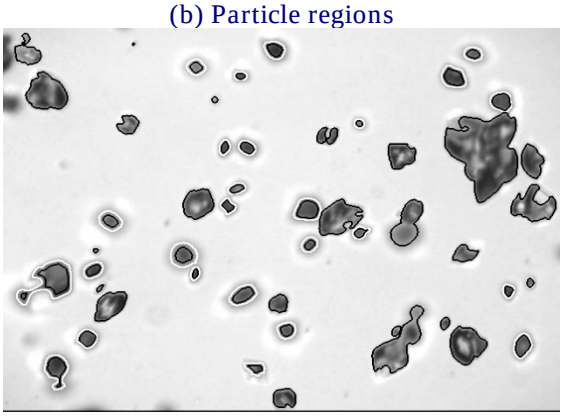

(d) In black, clean and deconvolved particles (particles used to compute the CSD); in white, blurred particles of image (c). Clean particles are not deconvolved

Figure 2: Image processing algorithm

IV. Results

Crystallization experiments were performed in a 3L lab-scale batch jacketed crystallizer, equipped with a profiled pale propeller (Mixel TT) and four baffles. The stirring rate was set to 250 rpm. The temperature of the crystallizing suspension was controlled by means of hydro-alcoholic fluid circulating in the jacket. Isothermal desupersaturation crystallization

experiments were started though seeding: sieved citric acid particles were introduced in the crystallizer kept under supersaturated conditions. In addition to in situ image acquisition, the process was monitored thanks to in situ temperature and supersaturation measurements; the latter was performed using ATR FTIR spectroscopy.
(Figure 3(b)) shows typical results of CSD obtained after processing the "raw" image displayed in (Figure 3(a)) with the image processing algorithm explained in the previous section.
Both the CSD in the reactor and in the measurement cell are assumed to be homogeneously distributed thanks to stirring which maintains the particles in suspension. Five minutes after seeding (*i.e.* after crystallization is started), it can be observed that the majority of the particles still exhibit a diameter smaller than 100µm ((Figure 3(b)). However, it is worth noting that a peak is present around 136µm, which corresponds to the aggregated particle present in the bottom center of the image ((Figure 3(a)).

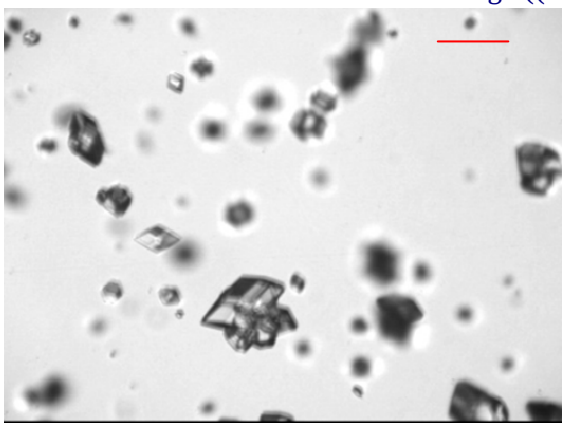

(*a*) 2D image of citric acid during crystallization at t=5min23s

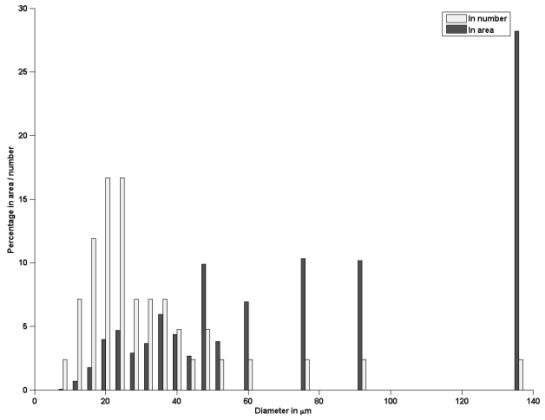

(b) CSD of citric acid at t=5min23s. In dark grey, CSD in area; in light grey CSD in number

Figure 3: CSD of citric acid particles at t=5min23s. The CSD are expressed in terms of percentage in projected area or number of particles.

Since only few particles can be observed on each image, an improvement of the CSD is obtained after averaging the CSD computed during a "short" period of time [t, t+Δt].

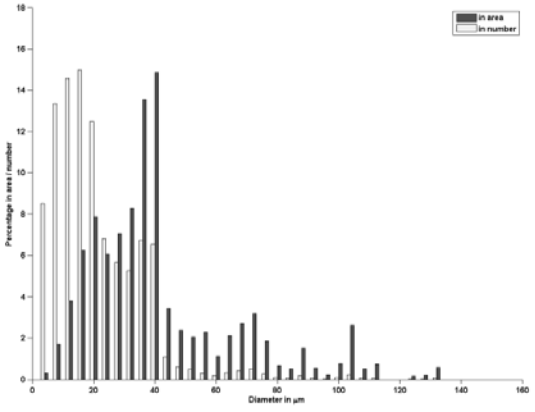

(*a*) Average CSD between [1min51s, 2min01s] In dark grey, average CSD in area; in light grey average CSD in number

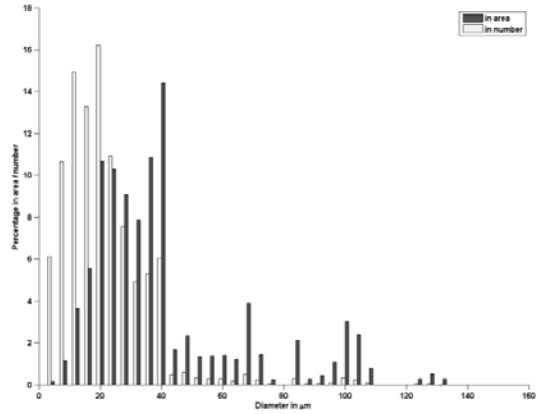

(b) Average CSD between [2min01s, 2min11s] In dark grey, average CSD in area; in light grey average CSD in number

Figure 4: Average CSD around t=2min01s

Appropriate choice of the sampling period Δt should be made so as to fulfill a satisfactory tradeoff between the accuracy of the "actual" estimates and the time-variations of the CSD. Moreover, it is usually considered that correct particle sampling requires at least 1000 particles to be "measured".

(Figure 4(a)) (*CSD_1*) shows the average CSD of citric acid computed during the period [1min51s, 2min01s] (10 seconds) and (Figure 2(b)) (*CSD_2*) shows the average CSD of citric acid during the consecutive period [2min01s, 2min11s] (10 seconds): the overall dynamics of the crystallization process is such that it can reasonably be assumed that no significant variation should be observed during the corresponding 10 seconds and more than 1000 particles should be analyzed.
Firstly, it is worth noting that, as expected, the estimated *CSD_1* and *CSD_2* look really similar. Secondly, from a more quantitative point of view, the average sizes computed from *CSD_1* (14.18µm in number and 27.88µm in area) and *CSD_2* (14.46µm in number and 27.25µm in area) are very close, which confirms that in 10 seconds, the particle sizes do not evolve significantly and the reproducibility of the estimates is satisfactory.
About 3min30s later, due to the development of both crystal nucleation and growth, the CSD spreads and the growth of the initial seed particles leads to the emergence of new CSD classes: [140µm, 240µm] (Figure 5).

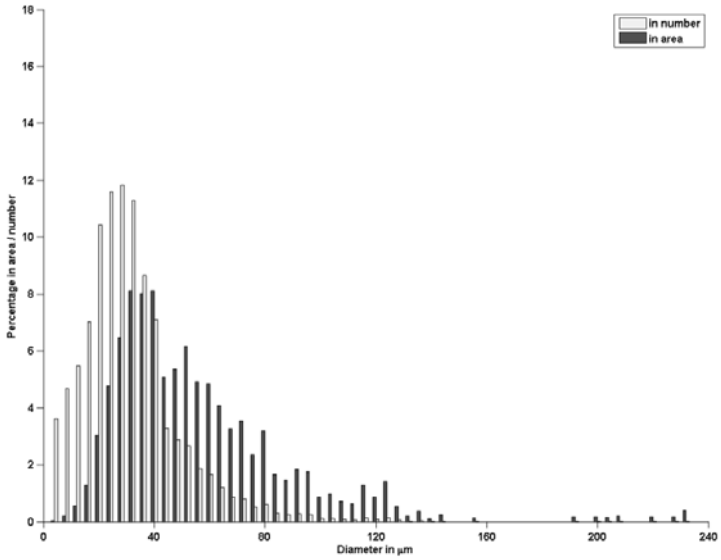

Figure 5 : Average CSD between [5min23s, 5min33s]. In dark grey, average CSD in area; in light grey average CSD in number

It is worth noting that the average CSD computed during the time interval [5min23s, 5min33s] is quite different from the CSD calculated at t=5min23s (Figure 3(b)). This is clearly because the set of particles processed to yield the “instantaneous CSD” at t=5min23s is too poor.
In addition to the size distribution, it should be noticed that shape parameters (elongation, convexity, etc.) can be calculated for each particle, providing information about possible anisotropy of the particles and aggregation processes.

V. Conclusions

During the present work, a new image analysis method allowing estimating the time-varying crystal size distribution of particles in suspension was developed and evaluated through crystallization experiments performed with citric acid in water. 2D images were acquired during the batch process using a new in situ imaging probe. The image analysis method is composed of three steps. A segmentation step allowed identifying each particle in the image. Thereafter, a restoration step was designed which enabled maximizing the number of particles that could be processed in a reliable way. Such goal was reached thanks to the deconvolution of blurred particles. Finally, the last step (particle measurement accomplished thanks to mathematical morphology) allowed obtaining the CSD all over the time (until moderate solid concentration).

The proposed image analysis method was implemented in Matlab® and all the computations were performed on a personal computer with 2 Ghz CPU and 512 Gb RAM running windows XP. With this computer set-up and without any optimization, the image analysis algorithm needs about 1 minute to complete the CSD of one image.
It is clear that such processing time is too large to allow real time CSD calculation. A conversion to the C language and a multi-cpu optimization could drastically improve it.
In conclusion, the present preliminary study provides a set of software tools yielding information on temporal changes of both two-dimensional particles geometry and crystal size distribution, which could enable improvements of the control of pharmaceutical crystallization processes.

Acknowledgment

We greatly acknowledge the French research agency ANR for the support granted to the project “IPAPI” (Improving the Properties of Active Pharmaceutical Ingredients), ref. 07-BLAN-0183

References

Beucher, S., 1992. The watershed transformation applied to image segmentation. *Scanning Microscopy International*, pp.299-314.

Fish, D.A., Brinicombe, A.M., Pike, E.R. & Walker, J.G., 1995. Blind deconvolution by means of the Richardson-Lucy algorithm. *Journal of the Optical Society of America A: Optics, Image Science, and Vision*, 12(1), pp.58-65.

Gonzalez, R. & Woods, R., 2002. *Digital Image Processing*. Prentice Hall.

Hukkanen, E. & Braatz, R., 2003. Measurement of particle size distribution in suspension polymerization using in situ laser backscattering. *Sensors and Actuators B: Chemical*, 96(1-2), pp.451-59.

Kundur, D. & Hatzinakos, D., 1996. Blind image deconvolution. *Signal Processing Magazine, IEEE*, 13(3), pp.43-64.

Kundur, D. & Hatzinakos, D., 1996. Blind image deconvolution revisited. *Signal Processing Magazine, IEEE*, 13(6), pp.61-63.

Mougin, P., 2003. Sensitivity of particle sizing by ultrasonic attenuation spectroscopy to material properties. *Powder Technology*, 134(3), pp.243-48.

Presles, B. et al., 2009. Monitoring the particle size distribution using image analysis during batch crystallization processes. In *Proceedings of the International Conference on Quality Control by Artificial Vision*. Wels, Austria, 2009.

Soille, P., 2003. *Morphological Image Analysis: Principles and Applications*. New York: Springer-Verlag.

Subbarao, M., Choi, T. & Nikzad, A., 1993. Focusing Techniques. *Journal of Optical Engineering*, 32, pp.2824-36.

Vincent, L., 1993. Morphological Gray Scale Reconstruction in Image Analysis: Applications and Efficient Algorithms. *IEEE Transactions on Image Processing*, 2(2), pp.176-201.

Wee, C.-Y. & Paramesran, R., 2007. Measure of image sharpness using eigenvalues. *Information Sciences*, 177(12), pp.2533-52.

Worlitschek, J., Hocker, T. & Mazzotti, M., 2005. Restoration of PSD from Chord Length Distribution Data using the Method of Projections onto Convex Sets. *Particle & Particle Systems Characterization*, 22(2), pp.81-98.

Yap, P. & Raveendran, P., 2004. Image focus measure based on Chebyshev moments. 151, pp.128-36.

Zhou, Y., Srinivasan, R. & Lakshminarayanan, S., 2008. Critical evaluation of image processing approaches for real-time crystal size measurements. *Computers & Chemical Engineering*, 33(5), pp.1022-35.